Ultrasonics - Sonochemistry 51 (2019) 186–196

Contents lists available at ScienceDirect

Ultrasonics - Sonochemistry

journal homepage: www.elsevier.com/locate/ultson

Conformational and physicochemical properties of quinoa proteins affected by different conditions of high-intensity ultrasound treatments

A. Vera[a], M.A. Valenzuela[b], M. Yazdani-Pedram[b], C. Tapia[a,*], L. Abugoch[a,*]

[a] Departamento de Ciencia de los Alimentos y Tecnología Química, Facultad de Ciencias Químicas y Farmacéuticas, Universidad de Chile, Santos Dumont 964, Santiago, Chile

[b] Facultad de Ciencias Químicas y Farmacéuticas, Universidad de Chile, Sergio Livingstone 1007, Santiago, Chile

ARTICLE INFO

Keywords:
High-intensity ultrasound
Pulses on-off
Quinoa proteins
Conformational structure
Physicochemical properties

ABSTRACT

Quinoa proteins (QP) have promise as a potential source of novel food ingredients, and it is of great interest to know how high-intensity ultrasound (HIUS) treatments affect the properties of QP. This work aimed to study the impact of on-off time-pulses of HIUS treatments on the structural and physicochemical properties of QP; samples were treated at 5, 10, 20, and 30 min with on-off pulses of 10 s/10 s, 5 s/1 s, and 1 s/5 s). Structural changes were evaluated using PAGE-SDS, circular dichroism, fluorescence spectroscopy, and differential scanning calorimetry. Meanwhile, physicochemical properties were also examined, including solubility, Z-average, polydispersity index PDI, and Z-potential. PAGE-SDS showed the appearance of polypeptides over 190 kDa in HIUS samples-treated. All samples presented 15.6% α-helices, 31.3% β-sheets, 21.8% β-rotations, and 31.4% random coils independent of the HIUS treatment. β-Turn structures and "random coils" were not affected by HIUS. When US 10 s/10 s and 1 s/5 s were applied, an increase in the % α-helix and a decrease in β-fold were observed, which could indicate a small conversion of β-folds to α-helices. Fluorescence spectra for all HIUS showed a significant increase (23%) of average fluorescence intensity and a decrease of λmax in relation to that of the control (346 dnm and 340 nm average HIUS treatment). DSC showed one endotherm in all cases (81.6–99.8 °C), and an increase in Td was observed due to the effect of the HIUS treatment. HIUS caused a 48% increase in solubility. The Z-average of the HIUS samples compared to that of the controls showed an increase from 37.8 to 47.3 nm. PDI and Z-potential values from the QP controls and the HIUS samples did not show significance differences and presented average values of 0.466 ± 0.021 (PDI) and −16.63 ± 0.89 (Z-potential). It is possible to conclude that HIUS treatments affect the secondary and tertiary structure of quinoa proteins, and these changes resulted in an increase of solubility and particle size. HIUS treatment as a new and promising technology that can improve the QP solubility properties and in that way allow its use as an ingredient with a good source of protein to develop different types of beverages/protein sauces.

1. Introduction

Ultrasound technology has attracted considerable attention in recent years and has been extensively used in the processing of food in both liquid and solid media (1, 2). Its functional mechanism is based on passing waves that create regions of high and low pressure; this variation in acoustic pressure is directly proportional to the amount of energy applied to the system. Ultrasound can be classified into two categories: low intensity (1 W/cm^2) with a frequency of 5–10 MHz and high intensity (10–1000 W/cm^2) with a frequency of 20–100 kHz [3,4]. Moreover, high-intensity ultrasound (also known as power ultrasound) is an effective technology for modifying structural and functional properties of proteins [5], such as whey protein concentrate, soy protein isolate/concentrate, and egg white protein [6]. Ultrasound-induced protein modification is often attributed to acoustic cavitation. Cavitation-induced activities, such as high shear by micro- and macro-streaming, shock waves, and water jets, help to reduce the size of protein aggregates and alter the molecular structure of protein [7]. Previous studies have investigated the changes in molecular structure of proteins after high-intensity ultrasound (HIUS) treatment, which induced alterations in free sulfhydryl groups, particle sizes, surface hydrophobicity, and secondary structures [8] and an increase in intramolecular mobility and surface activity [9]. Similarly, Hu et al. [2] reported that ultrasonic treatment of soy proteins resulted in partial unfolding and a reduction of intermolecular interactions, as demonstrated by increases in free sulfhydryl groups and surface

* Corresponding authors.
E-mail addresses: ctapia@uchile.cl (C. Tapia), labugoch@uchile.cl (L. Abugoch).

https://doi.org/10.1016/j.ultsonch.2018.10.026
Received 1 August 2018; Received in revised form 3 October 2018; Accepted 19 October 2018
Available online 24 October 2018
1350-4177/

hydrophobicity, and this led to improved solubility and fluid characteristics of soy protein isolate (SPI) dispersions. When it is used ultrasound treatments with high levels of power output ~400 W it was observed some grade of unfolding of QP Li et al. [10].

Quinoa (*Chenopodium quinoa* Willd) is a South American dicotyledonous. Quinoa proteins represent ≈16% of total dry quinoa seeds and it has high nutritional value due mainly to their high content of good quality protein [10,11]. QP can provide technological functional properties that there are totally related to their structure. There is potential for the production of protein concentrates from dehulled quinoa seeds, which could be used as raw material in the food industry as a technological functional ingredient as edible films, beverage, sauces, sausages [11–13]. The main protein fractions in quinoa grain are albumins and globulin [14,15]. Brinegar et al. [14,15], studied the molecular structures of quinoa globulin and albumin and reported that both proteins are stabilized by disulfide bridges. According to our knowledge, little is known about the effects of HIUS treatment conditions on the structure of quinoa proteins, and furthermore, how this effect acts on the physical properties of quinoa proteins to improve its use in food industry applications. Thus, the objective of this study was to investigate the effects of HIUS treatment on the conformational and physicochemical properties of quinoa proteins, as a function of treatment time with ultrasound (5, 10, 20, and 30 min) and on/off pulses (10 s/10 s; 5 s/1 s; and 1 s/5 s).

2. Materials and methods

2.1. Plant material

Quinoa flour (*Chenopodium quinoa* Willd) was supplied by Sociedad Comercial Agrícola Promauka Limitada, Paredones, VI Region of Chile. The flour was stored at 4 °C until it was used. Protein concentration was determined by Kjeldahl, and the percentage of nitrogen was converted to crude protein by multiplying it by a factor of 5.85 [16].

2.2. Obtaining the quinoa protein extract (QP)

The quinoa flour was defatted for 24 h with hexane in a 10% (w/v) suspension with continuous stirring, then air-dried at room temperature, and finally stored at 4 °C until use. Defatted quinoa meal was suspended in distilled water, and the pH was adjusted to 8.0 with 1 N NaOH. The suspensions were stirred for 60 min at room temperature and then centrifuged at 21,000*g* for 30 min at 15 °C [13]. The supernatants were lyophilized (ILSHINBIOBASE, model FD5508) and subsequently stored at 4 °C until use, and labelled as QP. The soluble protein content was 2.34 ± 0.5 mg/mL [17].

2.3. High-intensity ultrasound (HIUS) treatment

A volume of 250 mL of fresh QP solution was obtained and sonicated for 5, 10, 15, 20 and 30 min, using a 20 kHz Sonicator (Q Sonica, Q700 USA) with a maximum power output of 700 W; the energy input was provided through a 1.27 cm diameter probe with an amplitude of 20%, which resulted in 39 W of power, as provided by the ultrasound manufacturer's instructions. Sweep cycles (1, 5, 10 s) and pulse ratios (on-time/off-time) were (16.7%, 50%, and 83.3%), that is, 1 s on-time/5 s off-time (1 s/5 s), 10 s on-time/10 s off-time (10 s/10 s), and 5 s on-time and 1 s off-time (5 s/1 s). The temperature was controlled by placing the sample container in a beaker with ice (~20 °C). Untreated (QP) and US-treated QP samples were lyophilized (QP-HIUS) (ILSHINBIOBASE, model FD5508) and subsequently stored at 4 °C until use. All the samples (QP and QP-HIUS) presented an average protein content of 47.2 ± 0.3 g/100 g [16].

2.4. Conformational analysis of quinoa proteins

2.4.1. Sodium dodecyl sulfate-polyacrylamide gel electrophoresis (SDS-PAGE)

Lyophilized samples of QP and QP-HIUS were analysed by electrophoresis was carried out according to the Laemmli method [18]. All electrophoresis analyses were performed on gel minislabs (Bio-Rad Mini Protean III Model; Bio-Rad, Hercules, CA, USA). Sodium dodecyl sulfate-polyacrylamide gel electrophoresis gels contained 12% (w/v) acrylamide in the resolving gel and 5% acrylamide in the stacking gel. The molecular mass standard was obtained from Thermo Scientific (PageRuler™ Prestained Protein Leader) and contained proteins of the following sizes: 10, 17, 26, 34, 43, 55, 72, 95, 130 and 180 kDa. The sample loading buffer contained 0.124 M Tris–HCl (pH 6.8), 15% (v/v) glycerol and 2% (w/v) SDS. For reducing conditions, 5% (v/v) of 2-ME was added, and samples were heated (100 °C for 3 min). Protein bands were stained with Coomassie Brilliant Blue R [18].

2.4.2. Circular dichroism (CD)

Solutions of lyophilized samples of QP and QP-HIUS were prepared at 0.2 mg/mL protein content in distilled water. The CD spectra were recorded in the far UV range (190–250 nm) with a spectropolarimeter (Jasco J-1500, Japan Spectroscopic) at 20 °C and a quartz cuvette with 1 mm optical path length; an interval of 5 nm and a scan speed of 50 nm/min were used. Four scanning acquisitions were accumulated and averaged to obtain the final spectrum [19] using the Spectra Manager 2® software to obtain the data. The CD data were expressed in terms of ellipticity (millidegrees). The software CONTIN was used to obtain the % of each secondary structure type [20–23].

2.4.3. Fourier transform infrared spectra (FTIR)

QP and QP-HIUS lyophilized were analysed on an Agilent Technologies, Model Cary 630 (USA) FTIR spectrometer system, coupled to an attenuated total reflectance (ATR) accessory, equipped with a single-reflection diamond crystal. Measurements were performed using ~50 mg of powdered samples, which was placed on the surface of the ATR crystal, and pressed with a flat-tip plunger. A total of 20 scans were taken in the wavenumber range of 400–4000 cm^{-1} at a resolution of 4 cm^{-1} using resolution Pro software version 2.5.5 (Agilent Technologies USA). Analysis was carried out at room temperature.

2.4.4. Fluorescence spectroscopy

It was prepared samples of QP and QP-HIUS lyophilized at 0.2 mg/mL protein content in distilled water [17]. Fluorescence measurements were performed on a PerkinElmer LS-50 B luminescence spectrometer at room temperature. The excitation wavelength was 270–290 nm, and the emission spectra were recorded as the average of two spectra from 310 to 500 nm at a scan speed of 30 nm/min [13].

2.4.5. Determination of surface hydrophobicity (Ho)

Surface hydrophobicity was measured according to Kato and Nakai and Li et al., [24,25] using the fluorescence probe 1-anilino-8-naphthalene-sulfonate (ANS) [26]. The lyophilized samples of QP and QP-HIUS were diluted with distilled water to obtain concentrations of 0.2 mg/mL [17]. Then, 10 μL of ANS (8.0 mM in distilled water) was added to 3 mL of diluted sample, and the blends were incubated (~25 °C) for approximately 1 h [27]. The relative fluorescence intensity was determined using a Cary Eclipse Fluorescence Spectrophotometer at 390 nm (excitation wavelength, slit 10 nm) and 400–600 nm (emission wavelength, slit 5 nm). Three scanning acquisitions were accumulated and averaged to obtain the final spectrum. Surface hydrophobicity of the sample was expressed as the relative fluorescence intensity obtained with the 0.2 mg/mL protein concentration.

2.4.6. UV–VIS spectroscopy

The ultraviolet–visible (UV–Vis) spectra of the sample solutions (QP

and QP-HIUS lyophilized were prepared at 1 mg protein/mL in distilled water) were recorded ranging from 220 to 500 nm, using a spectrophotometer (Agilent 8453, Germany) at 25 °C with a 1 cm path length quartz cell.

2.4.7. Differential scanning calorimetry (DSC)

Differential scanning calorimetry (DSC131 EVO calorimeter, France) was used to determine the peak degradation temperature (Td) and associated energy of the thermal process, for both QP and QP-HIUS samples. Approximately 2 mg of each sample (QP and QP-HIUS lyophilized) was accurately weighed into aluminium pans and hermetically sealed. An empty pan was used for reference. The scanning temperature was raised from 20 to 140 °C at a rate of 10 °C/min [1,6]. The temperature at maximum heat flow of the endothermic transition and the area underneath the peak from the endothermal curve (J/g) were calculated.

2.5. Physicochemical analysis of quinoa proteins

2.5.1. Dynamic light scattering measurements

The particle hydrodynamic diameter (Z-average), polydispersity index (PDI), and Z-potential were measured at 25 °C using a Zetasizer Nano ZS-90 (Malvern Instruments, USA) operating at 4.0 mW and 633 nm with a fixed scattering angle of 173°. Soluble protein samples were prepared at a concentration of 10 mg of protein/mL [17] in Milli-Q ultrapure water, from QP and QP-HIUS lyophilized.

2.5.2. Determination of solubility

For this test, 10 mg of the sample (QP and QP-HIUS lyophilized) was dispersed in 1 mL of distilled water (1% w/w). The suspensions were stirred for 1 h and then centrifuged at 10,000 × *g* for 30 min at ± 20 °C. Soluble proteins were measured according to the Bradford method [17]. Solubility was expressed as a percentage of the total protein. Determinations were performed at least in triplicate.

2.6. Statistical analysis

All experiments were performed in triplicate, and each value represents the mean of at least two measurements from two independent ultrasound treatments. Significant differences in studied parameters between the control and HIUS-treated samples were determined by analysis of variance using the general linear model procedure (Statgraphics 3.0). An alpha level of 0.05 ($p < 0.05$) was used to determine significance. Statistically significant differences are indicated by the use of distinct superscripts.

3. Results and discussions

3.1. Conformational analysis of quinoa proteins

3.1.1. SDS-PAGE

SDS-PAGE profiles of the control QP and the samples treated at different HIUS time conditions can be observed in Fig. 1a–c, in the presence or absence of the reducing agent (2-ME). The non-reducing SDS-PAGE revealed molecular masses of the QP polypeptides were diffuse at 86, 66, 56, 27 kDa, and all protein bands less than 20 kDa are associated to albumin or 2S proteins components [14], those electrophoretic patterns were previously described [13,15,28]. It was observed that the band protein between 85 and 100 kDa was found more clear in all QP-HIUS than QP, this polypeptide was before already described [13,15,28]. The protein with MW 56 kDa was found in QP and in all QP-HIUS treatments and correspond to chenopodin or globulin 11S (Gl in the Fig. 1). Only HIUS-treated samples showed the appearance of polypeptides at MM greater than 190 kDa (HMWP in the Fig. 1), the formation of polypeptides of HMM from soy protein isolates induced by HIUS treatment was described by Tang et al. [29]. When analysing SDS-

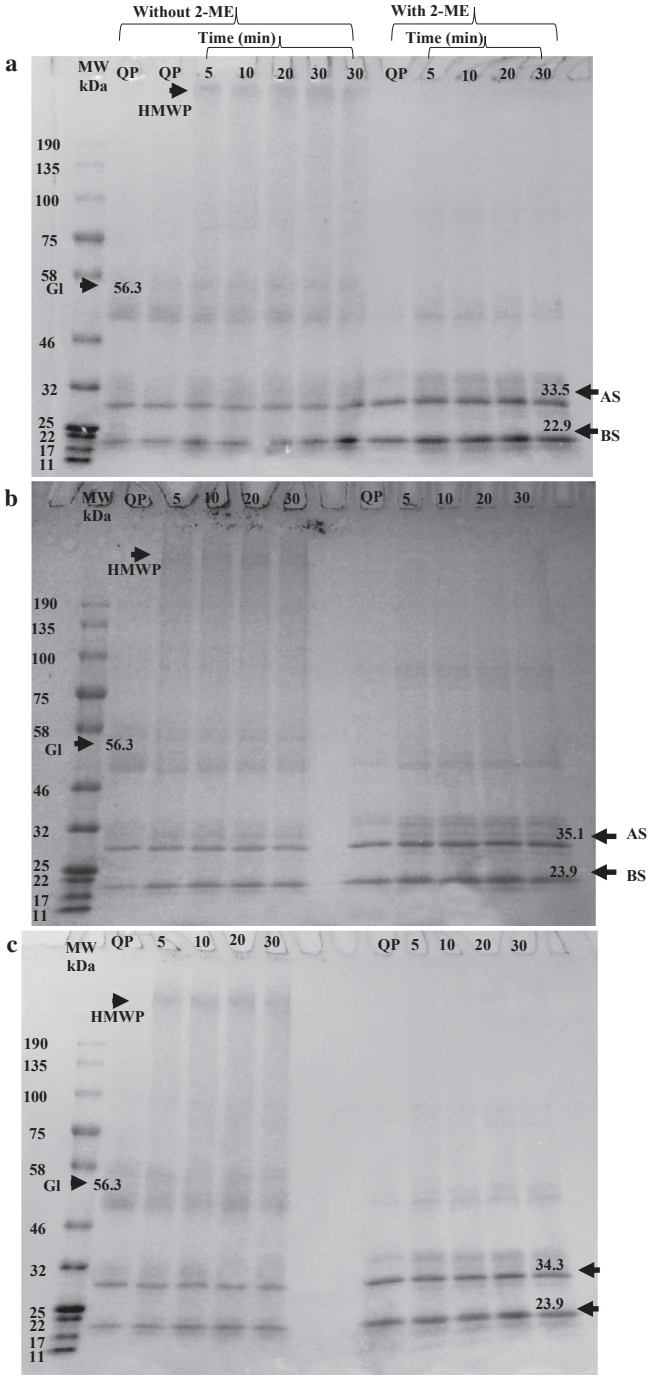

Fig. 1. Sodium dodecyl sulfate-polyacrylamide gel electrophoresis of control (QP) and high-intensity ultrasound (QP-HIUS) treatments of quinoa proteins under non-reducing and reducing (with 2-ME) conditions. a. QP-HIUS 10 s/10 s. b. QP-HIUS 5 s/1 s. c. QP-HIUS 1 s/5 s. Where PHMM is the polypeptide of high molecular weight; Gl correspond to globulin 11S; AS means acid subunit; and BS is the basic subunit.

PAGE results of the QP, QP-HIUS polypeptides in the presence of the reducing agent, a greater intensity was observed in the area close to ~35 kDa (associated with the acid subunit) and another in the zone of ~22 kDa (basic subunit); this band indicates the presence of chenopodin, which showing that is stabilized by disulfide bridges, as previously described by others [15,31,32]. HMWPs of QP-HIUS samples (with 2-ME) disappear showing that are stabilized by disulphide bridges and could correspond to trimeric or hexameric structures that can adopt globulins 11S [31].

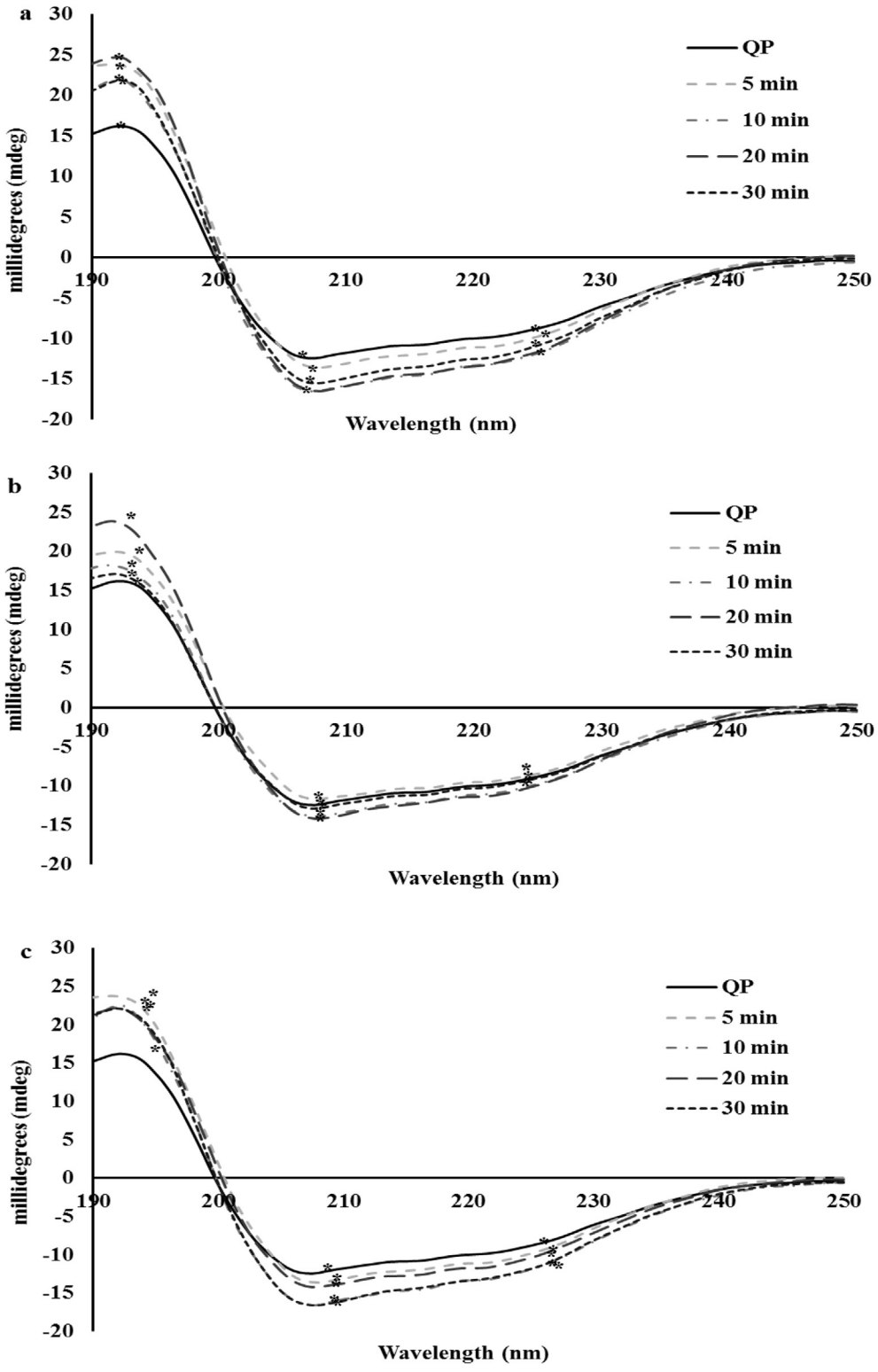

Fig. 2. Circular dichroism spectra of control (QP) and high intensity ultrasound (HIUS) treatments of quinoa proteins at 5, 10, 20 and 30 min with 20% amplitude by pulse ratios on-time/off-time a: HIUS 10 s/10 s; b: HIUS 5 s/1 s, and c: HIUS 1 s/5 s.

3.1.2. Circular dichroism (CD)

Chen et al. [32] utilized CD to assess the secondary structure of several proteins in the aqueous phase and identified two inflection points within the negative elliptic zone, approximately 222 and 209 nm, that indicate the presence of an α-helix, in addition to an ellipticity (+) maximum of approximately 192 nm. The control sample presented 15.6% α-helix, 31.3% β sheet, 21.8 β rotation and 31.4% random coil, which are similar to percentages reported by Mäkinen et al. [33] for alkaline extracts of quinoa proteins and to that described by Marcone et al. [34] for other proteins from dicotyledonous seeds. The CD results of the ultrasound-treated samples in addition to the control can be seen in Fig. 2. All collected spectra presented two minimal (negative) inflections (marked with * in the figure), one in the range of 206.5–208 nm and the other less negative inflection

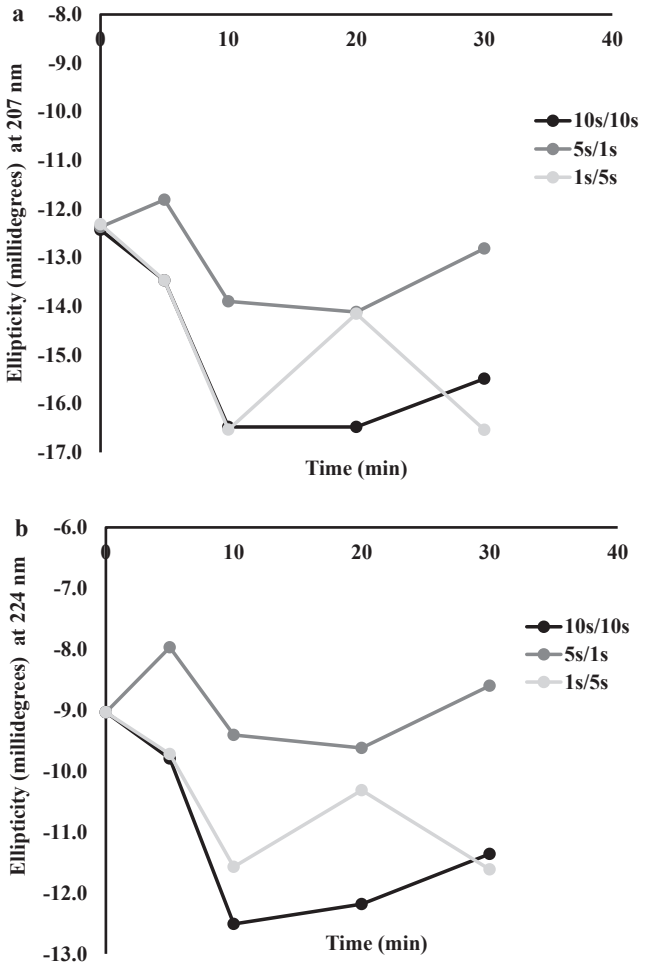

Fig. 3. Chance of ellipticity as a function of HIUS time treatments of quinoa proteins: (a) 207 nm y (b) 224 nm.

approximately 224.5–228.0 nm, in addition to a positive maximum at approximately 192.5 nm, which coincides with the ranges described by Chen et al. [32]. These ranges found for HIUS-treated quinoa proteins coincide with those described by Navarro-Lisboa et al. [35] for protein fractions at pH 7, showing that two negative values of ellipticity at 207 and 222 nm are associated with α-helix secondary structures; Choi and Ma [36] also associated these values to α-structure for buckwheat globulins. Fig. 3 shows the values of ellipticity at 207 nm (Fig. 3a) and at 224 nm (Fig. 3b); these values differ in all HIUS-treated samples compared with those of the control. Fig. 3a and b shows that the smallest fluctuations correspond to 5 s/1 s HIUS, while the largest fluctuations were shown by the 1 s/5 s treated samples. A great decrease in ellipticity related to that of the QP control was observed for the 10 s/10 s treated samples until a treatment duration of 10 min was reached, and subsequently, a tendency to remain constant was observed. The 10 s/10 s treatment caused the greatest change in ellipticity in relation to the control, which could be attributed to changes in secondary structure potentially associated with an unfolding in its structure [33]. Fig. 4a–c shows the determination of % secondary structure content for the control protein extract and those treated with ultrasound for varying durations (5, 10, 20 and 30 min) and treatment conditions (10 s/10 s, 5 s/1 s, and 1 s/5 s). Observed changes in the secondary structure may be associated with the sonication treatment. This treatment could cause the breakdown of interactions that stabilize this structural level such as hydrogen bonds and/or electrostatic interactions, and in some cases producing proteins unfolding (HIUS 10 s/10 s). Li et al. [10] reported that HIUS treatment at high power conditions (more than 200 W) changed the proportions of a-helix, b-sheet, b-turn, and random coil producing unfolding of QP, and showed that ultrasound treatment increased the random coil at high power (600 W).

3.1.3. Fourier transform infrared spectroscopy (FTIR)

Fig. 5 shows the FTIR spectra of the QP control and HIUS-treated samples. The main spectral observations were three intense bands attributed to amide I (~1600 cm^{-1}), amide II (~1500 cm^{-1}) and amide III (~1200 cm^{-1}) [37]. The comparison of FTIR spectra revealed differences between the control and HIUS-treated quinoa proteins [38]. All samples treated with HIUS for 5 min produced a decrease in the ~1600 cm^{-1} intensity band with respect to that of the QP control; moreover, the amide II and III bands remained without variation between the samples. At 10 min of HIUS 10 s/10 s treatment, an increase in all intensity bands was displayed, and the remaining HIUS treatments showed a decrease in the three amide zones, all compared to those of the control. Regarding samples treated with HIUS for 20 min, only the 5 s/1 s treatment showed a decrease in the three amide zones in respect to those of QP; and finally, when considering samples treated for 30 min, the 10 s/10 s treatment showed a notorious increase in amide I, II and III bands. In contrast, the 1 s/5 s and 5 s/1 s treatments showed a decrease in all amides zones compared to those of the QP control. The amide I zone revealed oscillations of the polypeptide structure related to C═O stretch vibrations, which has generally been associated with changes in the secondary protein structure [39], and which could correspond to C–O, N–H stretching caused by flexural vibration frequencies of the intra- and inter-molecular hydrogen bonds produced by the cavitation and energy provided by the HIUS treatment. In regards to samples treated with HIUS for 5 min, it is possible to observe an increase in the intensities of the amide I zone. The 10 s/10 s treatment exhibited higher variation in the amide I zone (at 10 and 30 min) [40]. The effect of starch on HIUS treatments was considered in the spectrum located between 1200 and 900 cm^{-1}, because in this is dominated by ring vibrations overlapped with stretching vibrations of (C–OH) side groups and the (C–O–C) glycosidic bond vibrations [41]. Quinoa seeds have around 60% of starch [42] with high content of amylose and amylopectin [43], so those polysaccharides consist of α(1–4)-linked glucose units but amylose is linear, and amylopectin is a highly branched polymer with α(1,4; 1,6)-linked glucose units. The FTIR spectrum (Fig. 5) show that QP/QP-HIUS has bands ~1098 cm^{-1} and 950 cm^{-1}, it was observed in some cases increase/decrease of those bands related to QP, these changes can be associated to the loss of molecular order of QP starch [44]. Since application of HIUS to liquid systems causes acoustic cavitation generating growing and eventual collapse of the bubbles, the US waves propagate, the bubbles oscillate and could cause collapse which could produce collapse pressure, turbulences, and shear stresses [45] and produce the QP unfolding observed, these observations in the FTIR spectra are in agreement with the CD data described in the previous section.

3.1.4. Fluorescence spectroscopy

Fluorescence is a useful technique to follow the transition of the tertiary structure in proteins since the intrinsic fluorescence of aromatic amino acid residues is sensitive to the polarity of the microenvironment [46]. The fluorescence spectrum of proteins is particularly attributed to the tryptophan residue [47] since the intensity of its spectrum is greater than that of phenylalanine and tyrosine [48]. Fig. 6 shows the fluorescence spectra corresponding to US treatments of differing duration (5, 10, 20, and 30 min) and pulse on-pulse off condition (10 s/10 s, 5 s/1 s, and 1 s/5s). All US conditions revealed a significant increase of ~23% in fluorescence intensity (FI) relative to that of the control. In contrast, it was also observed that the maximum wavelength (λmax) corresponding to different treatments of HIUS presented significant a decrease in relation to the control ($p < 0.05$), from 346 nm (control) to 340 for QPs treated with HIUS; this decrease indicates a blueshift and

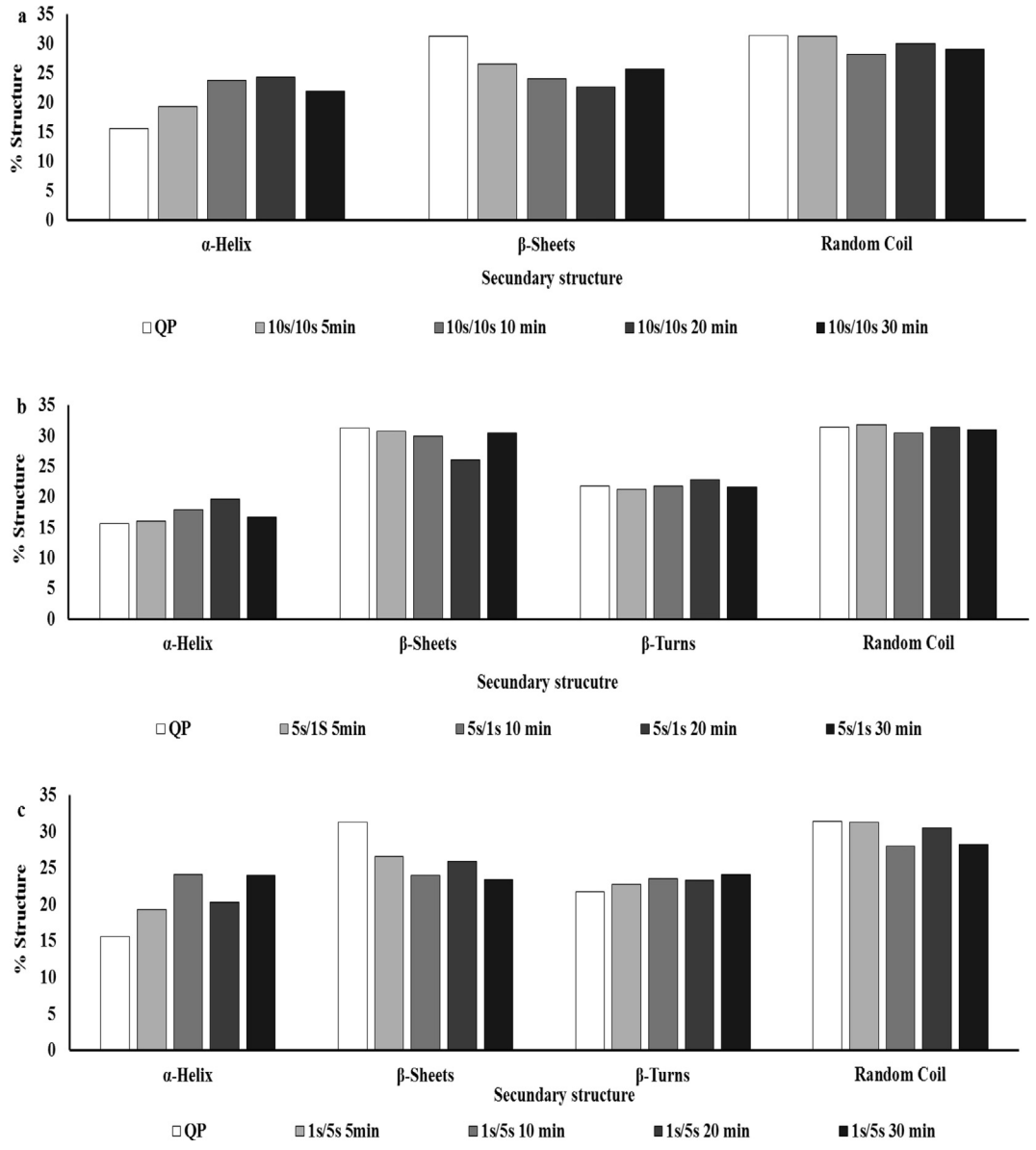

Fig. 4. Secondary structure % contents of control quinoa protein and those treated with ultrasound (HIUS) at 5, 10, 20 and 30 min by pulse ratios (on-time/off-time), a: 10 s/10 s; b: 5 s/1 s; and c: 1 s/5 s, estimated from circular dichroism spectra in the far-UV región (190–250 nm).

denominated hypsochromic effect [49]. The fluorescence of tryptophan (Trp) side chains in a protein is extremely sensitive to the environment; thus, observed changes in FImax and λmax are useful indicators of protein structural and conformational changes [2,6,50–52]. Three kinds of tryptophan residues have been described according their λmax emission: a value between 330 and 332 nm is considered a buried residue, 350–353 nm is considered exposed, and 340–342 is considered exposed with limited water contact and is likely immobilized at the surface [48]. For the QP control sample, values were ~346 nm indicating that Trp were mainly exposed, but for QP-HIUS, values were ~340 nm, indicating that Trp residues shifted towards being exposed with limited water contact, emitting a greater energy due to molecular conformational change into a more hydrophobic environment [49]. The structural changes caused by HIUS treatments on quinoa proteins could be due to cavitations generated when gas bubbles form and collapse due to pressure differences that occur in microseconds, causing shear forces and an increased temperature [8,53].

3.1.5. Determination of surface hydrophobicity (Ho)

Changes in the conformational structure of quinoa proteins were determined from measurements of extrinsic (ANS-binding) fluorescence (Fig. 7). The extrinsic fluorescence emission spectra of QP and HIUS-treated samples ranged from 473 to 472 nm; Zhang et al. [54] described a λmax of 467 nm of soy proteins binding to ANS-probes. In some cases, HIUS 10 s/10 s and 5 s/1 s treatments showed a slight blueshift of 1 nm in the emission wavelength, oscillating between 473 nm and 472 as shown in (Table 1). This behaviour was not observed during HIUS 1 s/5 s treatment conditions. Table 1 also lists the fluorescence intensities at λmax (FI). The FI of the HIUS US 10 s/10 s-treated sample significantly increased ($p < 0.05$) with respect to that of QP, and the sample treated for 20 min presented the highest value observed (221.57 ± 1.0). The HIUS US 5 s/1 s-treated samples presented increases and decreases in IF depending on the duration of treatment (Table 1), and the HIUS 1 s/5 s-treated samples showed a significantly decreased FI ($p < 0.05$) in relation to that of QP (control); furthermore, this treatment represented the smallest FI value observed, 147.0 ± 0.5. According to Stryer [55], the use of the probe ANS could be useful in detecting changes in the tertiary/quaternary structure of proteins, and interactions between ANS and hydrophobic binding sites within proteins are associated with two observations including a blueshift in the maximum peak and an

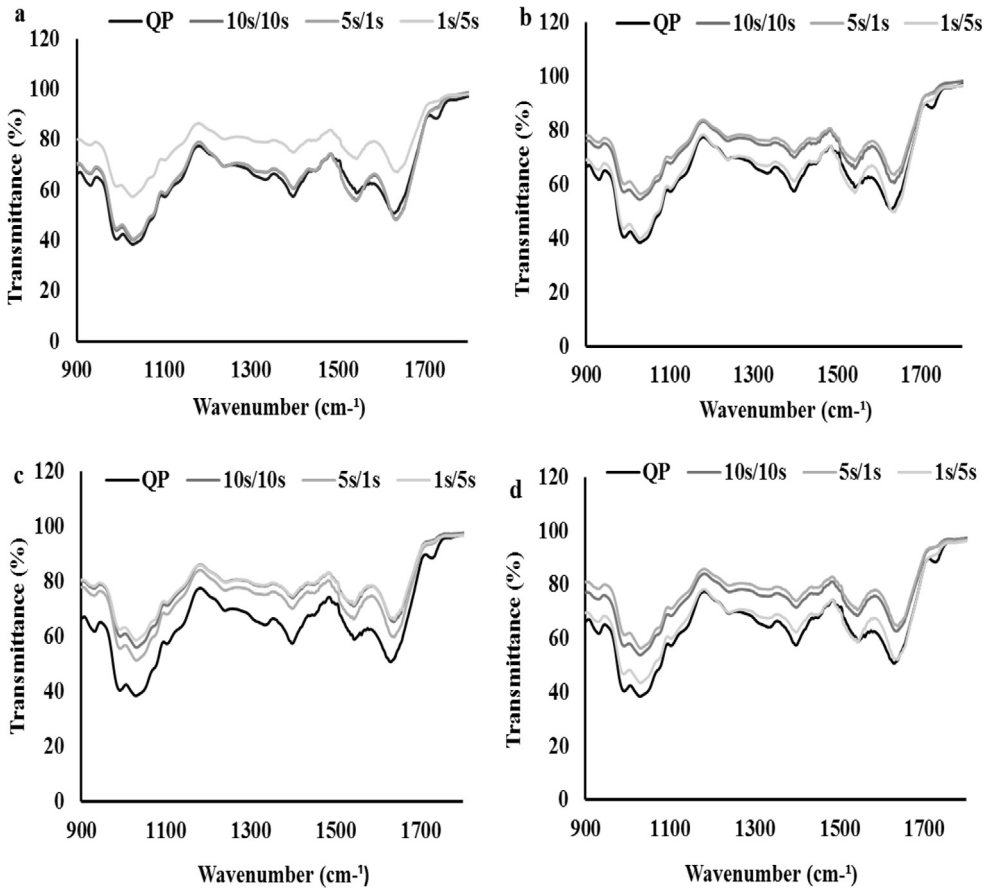

Fig. 5. FTIR spectra of control quinoa protein and those treated with ultrasound (HIUS) at a: 5 min, b: 10 min, c: 20 min and d: 30 min (pulse ratios (on-time/off-time), 10 s/10 s; 5 s/1 s; and 1 s/5 s).

increase in fluorescence [55]; ANS can therefore be useful for the detection of protein aggregation, folding, unfolding [55,56]. Notably, our results presented an increase an FI and a slight blueshift, primarily in samples that underwent HIUS US 10 s/10 s and 5 s/1 s treatments compared with those of the control. The conformational changes that may be attributed to the formation of HMWP of quinoa proteins [55,57]. In contrast, for the 1 s/5 s treated samples, a decrease in FI values was observed compared with that of the control, but no changes in λmax, which may suggest some degree of protein folding [55].

3.1.6. UV spectroscopy

UV spectra in the 250–320 nm region provide information about the tertiary structure of proteins [58] because aromatic chains of tyrosine (Tyr), tryptophan (Trp) and phenylalanine (Phe) absorb in the UV–visible region between 240 and 300 nm; these residues are sensitive to environmental modifications, so their absorption spectra can change in regards to both absorption and maximum wavelength [59]. In Fig. 8, spectra of HIUS-treated quinoa proteins and the untreated control are shown. Samples subjected to HIUS treatment had a significant change in λmax ($p < 0.05$) from 256 (non-treated) to 260 nm (HIUS-treated). According to Schmidt [59], denaturation occurs due to external agents when a small increase in wavelength associated with aromatic residues (Tyr, Trp, Phe) is observed [58,59], and quinoa globulin 11S contains aromatic residues [22,23]; thus, these results are to some degree suggesting that denaturation of quinoa proteins is occurring due to HIUS treatment. Absorbance values at λmax were ~1.96 ± 0.06 (control and all HIUS conditions). These absorbance values were not significantly different from that of the control, except for the HIUS 10 s/10 s treatment for 20 min that differed significantly from that of the other conditions and treatment durations ($p < 0.05$), presenting the highest absorbance value of 2.31 ± 0.01; this result may indicate a greater degree of unfolding and higher exposure of the aromatic residues [56]. In contrast, it is plausible that protein soluble of HMM formed, since an absorbance reading remains at 320 nm. Accordingly, positive differences were found between absorbances at 280–320 nm in a non-linear behaviour, which could further explain the degree of denaturation in HIUS-treated quinoa proteins (Fig. 8).

3.1.7. Differential scanning calorimetry (DSC)

DSC thermograms of quinoa proteins treated with HIUS and the untreated control are shown in Fig. 9. Observation of one endotherm in all cases is possible; these endothermic selections ranged from 81.6 to 99.8 °C (Fig. 9). This result could be associated with 11S globulins, since they make up the highest fraction at pH 8 [60]; this is also in agreement with other studies [13,61]. With this respect, these ranges can vary depending on the matrices and extraction conditions. For quinoa flour, a Td of ~98.9 °C was described [62], and for protein isolates at different pH values, the Tds varied between 96 and 102 °C [61]. Td values of quinoa proteins, presented a significant increase ($p < 0.05$) with the US treatment in relation to the control, except those treated at 10 s/10 s for 20 min and at 1 s/5s for 5 min, which were not significantly different. Seemingly, some HIUS treatments may contribute to the thermal stability of quinoa proteins. As 11S globulin is the main storage protein of quinoa seeds (and it is soluble at pH 8 [15,63]), also it is a hexamer protein with a MM of 320 kDa, of which each subunit consists of a basic peptide (20–25 kDa) and acid (30–40 kDa) covalently linked by an SS bond, and is a member of the highly conserved 11S storage globulin family [15,64]. We believe that 11S globulin can be affected by HIUS adopting trimeric conformations (~160 kDa) and/or hexamerics (~330 kDa), and it is in this sense that we are discussing, and thinking

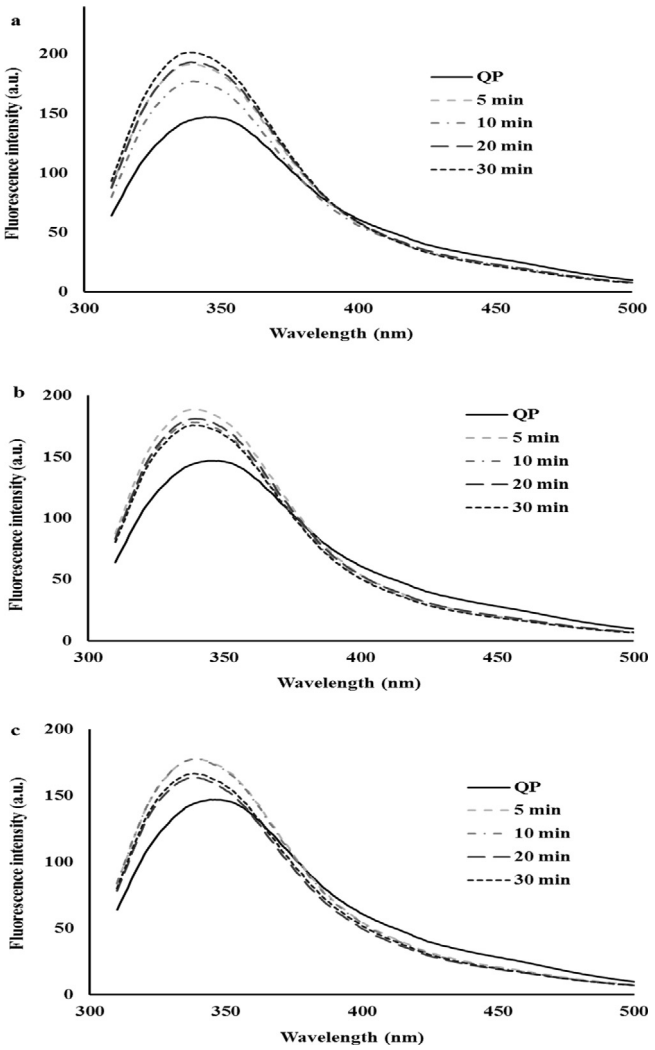

Fig. 6. Intrinsic fluorescence spectra of control quinoa protein and those treated with ultrasound (HIUS) at 5, 10, 20 and 30 min by pulse ratios (on-time/off-time), a: 10 s/10 s; b: 5 s/1 s; and c: 1 s/5 s.

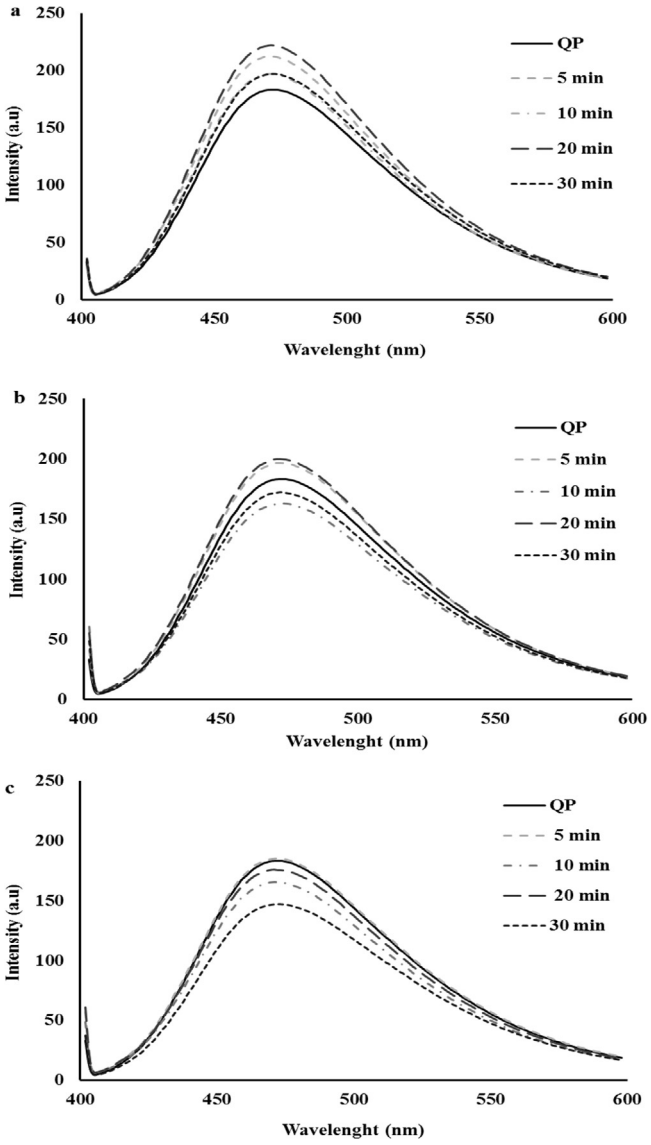

Fig. 7. Extrinsic fluorescence spectra of control quinoa protein and those treated with ultrasound (HIUS) at 5, 10, 20 and 30 min by pulse ratios (on-time/off-time), a: 10 s/10 s; b: 5 s/1 s; and c: 1 s/5 s.

that the increase in the particle size of its monomeric conformation (~55 kDa) to trimeric/hexameric since this conformations are stabilized by hydrophobic bonds between monomeric protein [65]. Karki [66] did not find a clear correlation between HIUS and the thermal behaviour of soy proteins. However, Malik et al. [65] studied denaturation of sunflower protein isolate induced by HIUS, and they found an increase of Td at ~30 min of HIUS treatment.

3.2. Physicochemical analysis of quinoa proteins

3.2.1. Dynamic light scattering measurements

The changes produced by HIUS of the proteins in QP was evaluated by dynamic light scattering, the polydispersity index (PDI) and Z-Potential. The HIUS-treated quinoa and control samples did not present significant differences in these values. The Z-potential ranged from −15.9 to −18.1 (average −16.6 ± 30.89). PDI values ranged between 0.471 and 0.485 (average 0.466 ± 0.021) (see Table 2); PDI is used to estimate the size distribution of a particle solution, a sample solution can be monodisperse when the PDI value is less than 0.1 [67], so these results are indicating that QP and QP-HIUS are polydisperse, and it could correspond to different levels of globulin11S [31]. The US 1 s/5 s presented slightly lower values ($p > 0.05$) of −15.3 to −15.6 and 0.414–0.456 (Z-potential and PDI, respectively). PDI in this research, did not show great changes due to HIUS; Z-potential was uniformly negative indicating that the surface ionic charge remained negative, which is expected due to the pH of the protein extraction solution (pH 8). The mean hydrodynamic diameters of the HIUS-treated

Table 1
Fluorescence intensity (FI) and λmax obtained from the extrinsic fluorescence emission spectra of quinoa protein control and HIUS-treated samples.

Time (min)	10 s/10 s	5 s/1 s	1 s/5 s
	λ_{max}		
0	473.0 ± 0.00	473.0 ± 0.00	473.0 ± 0.00
5	472.0 ± 0.00	472.0 ± 0.00	473.0 ± 0.00
10	472.0 ± 0.00	473.0 ± 0.00	473.0 ± 0.00
20	473.0 ± 0.00	472.0 ± 0.00	473.0 ± 0.00
30	473.0 ± 0.00	473.0 ± 0.00	473.0 ± 0.00
	FI		
0	183.24 ± 0.06	183.24 ± 0.06	183.24 ± 0.06
5	212.03 ± 0.18	196.36 ± 0.71	185.29 ± 0.13
10	197.17 ± 0.33	162.98 ± 0.50	165.28 ± 0.49
20	221.57 ± 0.99	199.84 ± 0.24	175.83 ± 0.35
30	197.09 ± 0.58	171.96 ± 0.59	146.95 ± 0.53

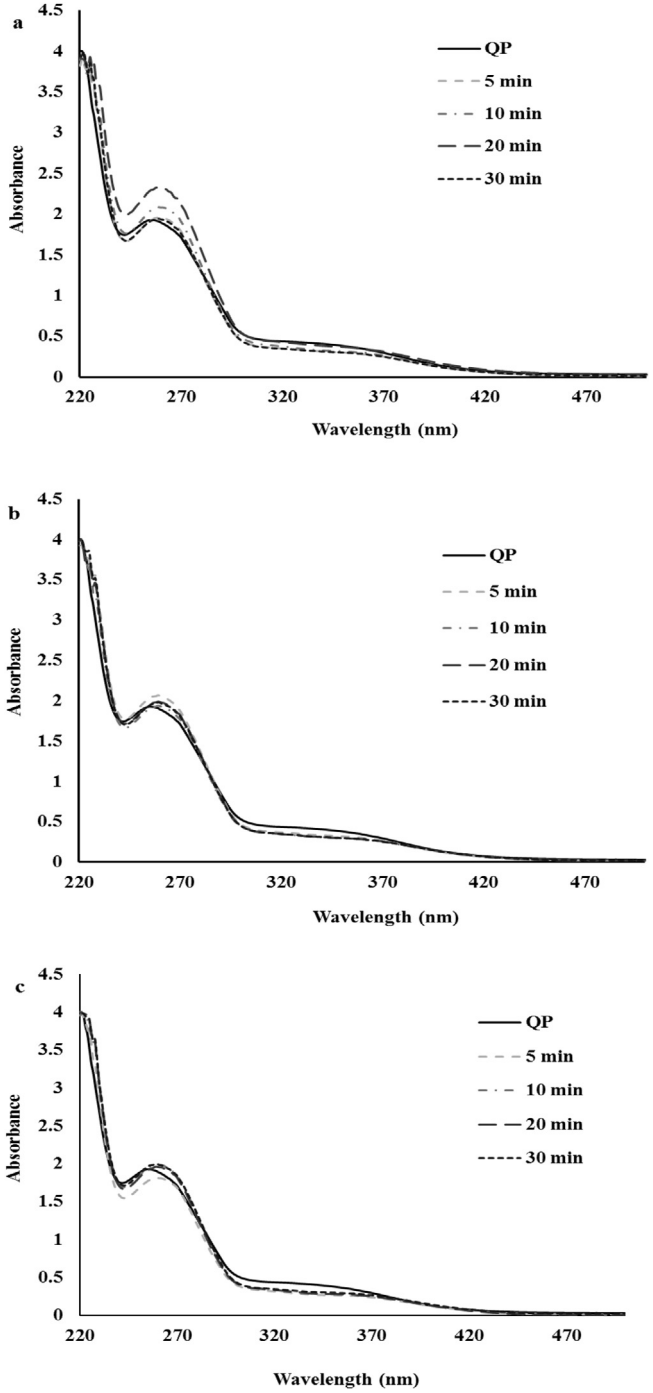

Fig. 8. UV–Visible spectra of control quinoa protein and those treated with ultrasound (HIUS) for 5, 10, 20 and 30 min by pulse ratios (on-time/off-time), a: 10 s/10 s; b: 5 s/1 s; and c: 1 s/5 s.

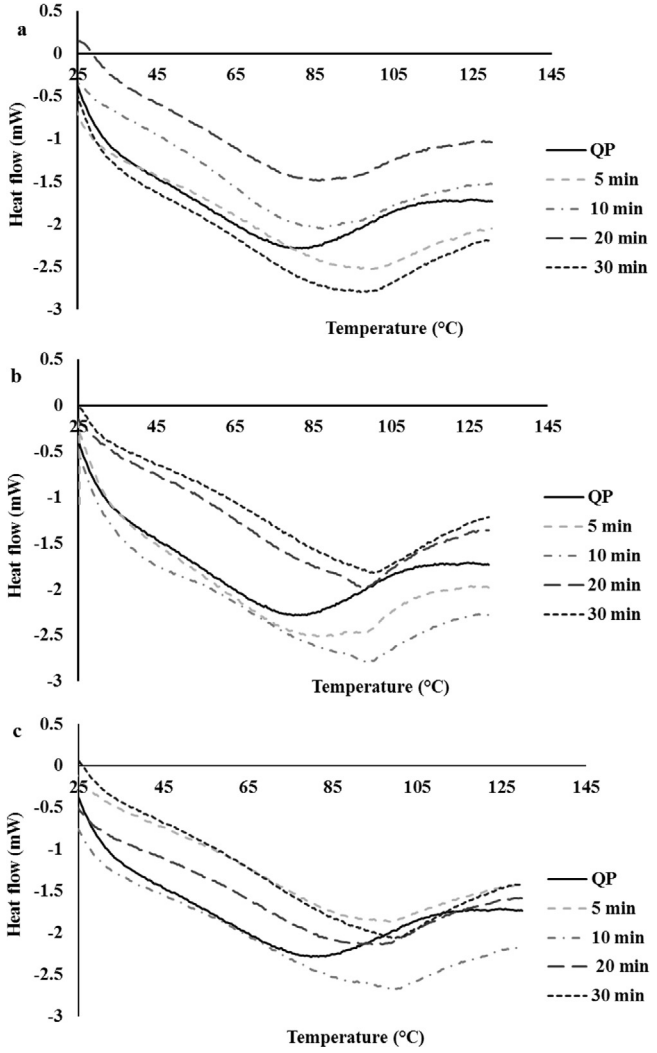

Fig. 9. DSC thermograms of control quinoa protein and those treated with ultrasound (HIUS) for 5, 10, 20 and 30 min by pulse ratios (on-time/off-time), a: 10 s/10 s; b: 5 s/1 s; and c: 1 s/5 s.

protein (Table 2) were between 40 and 46 nm and the non-treated sample was 38 nm. The mean hydrodynamic diameter (Z-average) of the HIUS-treated quinoa proteins increased compared to that of the control, which may indicate some aggregation of the treated proteins. Malki et al. [65] observed an increase in mean particle size at 30 min of HIUS, and they explain this increase in particle size indicates the aggregation of protein; also for BSA proteins at 40 min of HIUS treatment reported the particle size was increased, that indicates formation of small aggregates [8]. Z-average values ($p < 0.05$) were significant for all tested time durations for US 10 s/10 s and US 5 s/1 s but only at 30 min for US 1 s/5s; the Z-average did not present a significant difference compared to that of the QP control. This was consistent with the SDS-PAGE analysis of the proteins (Fig. 1) and UV spectra, suggesting that HIUS treatments could be favourable for the formation of quinoa soluble polypeptides of HMM, these polypeptides may be related to the trimeric or hexameric globulin 11S structure [31,68].

3.2.2. Solubility

The solubility of quinoa proteins is shown in Table 3; the solubility of the PE control (obtained at pH 8) was 44.3 ± 2.2%. Accordingly, Steffolani et al [30] showed that protein solubility depends not only on the pH but also on the specific quinoa variety from which the protein is derived; they described solubility values of quinoa protein isolates (obtained at pH 9) ranging from ~47 to 70% at neutral pH. Additionally, we observed that protein solubility increased ($p < 0.05$) after 5 min of HIUS treatments from 59.3 to 86.5%. US 10 s/10 s and US 5 s/1 s presented higher values than US 1 s/5 s (73.3 ± 2.9, 86.5 ± 10.7, and 59.3 ± 5.3%, respectively); this increase in solubility is related to the identified conformational changes and the formation of soluble HMWP, as observed previously in -SDS-PAGE and UV spectra [6,69]. After 5 min of treatment, the increased solubility typically remained and continued to rise, especially HIUS 1 s–5 s (Table 3). The resulting solubility following all treatments significantly differed compared to that of the control ($p < 0.05$). When considering that the

Table 2
Mean hydrodynamic diameter (Z-average) and polydispersity index (PDI) of quinoa proteins control and treated with HIUS.

Times (min)	Z-Potential			PDI		
	10 s/10 s	5 s/1s	1 s/5s	10 s/10 s	5 s/1s	1 s/5s
0	37.78 ± 3.75 ^{a}	37.78 ± 3.75^{a}	37.78 ± 3.75^{b}	0.47 3 ± 0.034^{a}	0.473 ± 0.034 ^{a}	0.473 ± 0.034^{a}
5	41.96 ± 9.16^{b}	47.29 ± 4.67^{b}	43.13 ± 4.09^{b,c,d}	0.470 ± 0.041^{a}	0.481 ± 0.032^{a}	0.414 ± 0.062^{a}
10	43.97 ± 6.99^{b}	45.41 ± 4.70^{b}	44.50 ± 11.85^{c,b,d}	0.479 ± 0.030^{a}	0.483 ± 0.022^{a}	0.442 ± 0.069^{a}
20	42.35 ± 6.00^{b}	46.02 ± 5.44^{b}	42.06 ± 5.15^{d,b,c,e}	0.468 ± 0.040^{a}	0.481 ± 0.028^{a}	0.456 ± 0.048^{a}
30	43.84 ± 5.94^{b}	45.76 ± 2.18^{b}	39.97 ± 3.18^{a,e}	0.485 ± 0.040^{a}	0.479 ± 0.030^{a}	0.426 ± 0.026^{a}

Different letters are significantly different ($p < 0.05$) between rows.

Table 3
Solubility of quinoa protein control and HIUS-treated samples.

Time (min)	10 s/10 s	5 s/1 s	1 s/5 s
0	2.33 ± 0.29^{a}	2.33 ± 0.29^{a}	2.33 ± 0.29^{a}
5	3.46 ± 0.91^{b}	3.93 ± 0.89^{b}	2.80 ± 0.86^{a,e}
10	3.35 ± 0.59^{b}	3.36 ± 0.98^{b}	3.33 ± 1.11^{b,e,f,g}
20	3.35 ± 0.38^{b}	3.56 ± 0.64^{b}	3.63 ± 0.76^{c,f,h}
30	3.26 ± 0.82^{b}	3.48 ± 0.43^{b}	3.85 ± 0.29^{d,g,h}

Different letters indicate significant difference ($p < 0.05$) between rows.

solubility of vegetable proteins increased after different HIUS treatments, as other authors have described [6,69], and that ultrasound treatment US 5 s/1 s produced a strong increase in the solubility of quinoa proteins, it seems that the pulse-on/pulse-off method could be an important variable to consider when HIUS is applied to increase quinoa protein solubility.

4. Conclusions

HIUS treatments of QP resulted in time-dependent conformational and physicochemical changes. HIUS treatments can be related to the formation/dissociation of trimeric and/or hexameric structures of globulin 11S. On the other hand, it seems that a small conversion of β-folds to α-helices occurs at the secondary structure level. Changes in the tertiary conformation of quinoa proteins were also observed, and some HIUS treatments were able to contribute thermal stability of the quinoa proteins. Conformational changes are related to physicochemical properties because a small increase in the size and in the solubility of quinoa proteins was observed in HIUS-treated samples. These results are applicable to the potential development of quinoa proteins for new ingredients and functional foods.

Acknowledgements

Projects INNOVA CORFO 12IDL2-13621, Fondequip EQM140151.

Appendix A. Supplementary data

Supplementary data to this article can be found online at https://doi.org/10.1016/j.ultsonch.2018.10.026.

References

[1] J. Chandrapala, B. Zisu, M. Palmer, S. Kentish, M. Ashokkumar, Effects of ultrasound on the thermal and structural characteristics of proteins in reconstituted whey protein concentrate, Ultrason. Sonochem. 18 (2011) 951–957, https://doi.org/10.1016/j.ultsonch.2010.12.016.
[2] H. Hu, J. Wu, E.C.Y. Li-Chan, L. Zhu, F. Zhang, X. Xu, G. Fan, L. Wang, X. Huang, S. Pan, Effects of ultrasound on structural and physical properties of soy protein isolate (SPI) dispersions, Food Hydrocolloids 30 (2013) 647–655, https://doi.org/10.1016/j.foodhyd.2012.08.001.
[3] J.A. Gallego-Juarez, High-power ultrasonic processing: recent developments and prospective advances, Phys. Proc. 3 (2010) 35–47, https://doi.org/10.1016/j.phpro.2010.01.006.
[4] T.S. Awad, H.A. Moharram, O.E. Shaltout, D. Asker, M.M. Youssef, Applications of ultrasound in analysis, processing and quality control of food: a review, Food Res. Int. 48 (2012) 410–427, https://doi.org/10.1016/j.foodres.2012.05.004.
[5] L. Chen, J. Chen, J. Ren, M. Zhao, Effects of ultrasound pretreatment on the enzymatic hydrolysis of soy protein isolates and on the emulsifying properties of hydrolysates, J. Agric. Food Chem. 59 (2011) 2600–2609, https://doi.org/10.1021/jf103771x.
[6] C. Arzeni, K. Martínez, P. Zema, A. Arias, O.E. Pérez, A.M.R. Pilosof, Comparative study of high intensity ultrasound effects on food proteins functionality, J. Food Eng. 108 (2012) 463–472, https://doi.org/10.1016/j.jfoodeng.2011.08.018.
[7] G.T.K. Weiss, K. Kristbergsson, Engineering food ingredients with high-intensity ultrasound, in: J.W.H. Feng, V. Barbosa-Canovas (Eds.), Ultrasound Technol. Food Bioprocess, Springer, New York, 2011.
[8] I. Gülseren, D. Güzey, B.D. Bruce, J. Weiss, Structural and functional changes in ultrasonicated bovine serum albumin solutions, Ultrason. Sonochem. 14 (2007) 173–183, https://doi.org/10.1016/j.ultsonch.2005.07.006.
[9] D. Güzey, I. Gülseren, B. Bruce, J. Weiss, Interfacial properties and structural conformation of thermosonicated bovine serum albumin, Food Hydrocolloids 20 (2006) 669–677, https://doi.org/10.1016/j.foodhyd.2005.06.008.
[10] X. Li, S. Da, C. Li, F. Xue, T. Zang, Effects of high-intensity ultrasound pretreatment with different levels of power output on the antioxidant properties of alcalase hydrolyzates from Quinoa (Chenopodium quinoa Willd.) protein isolate, Cereal Chem. 95 (2018) 518–526, https://doi.org/10.1002/cche.10055.
[11] C. Valenzuela, L. Abugoch, C. Tapia, Quinoa protein-chitosan-sunflower oil edible film: mechanical, barrier and structural properties, LWT – Food Sci. Technol. 50 (2013) 531–537, https://doi.org/10.1016/j.lwt.2012.08.010.
[12] L.E. Abugoch, C. Tapia, M.C. Villamán, M. Yazdani-Pedram, M. Díaz-Dosque, Characterization of quinoa protein-chitosan blend edible films, Food Hydrocolloids 25 (2011) 879–886, https://doi.org/10.1016/j.foodhyd.2010.08.008.
[13] L.E. Abugoch, N. Romero, C.A. Tapia, J. Silva, M. Rivera, Study of some physicochemical and functional properties of quinoa (*Chenopodium quinoa* Willd) protein isolates, J. Agric. Food Chem. 56 (2008) 4745–4750, https://doi.org/10.1021/jf703689u.
[14] C. Brinegar, B. Sine, L. Nwokocha, High-cysteine 2S seed storage proteins from quinoa (*Chenopodium quinoa*), J. Agric. Food Chem. 44 (1996) 1621–1623, https://doi.org/10.1021/jf950830+.
[15] C. Brinegar, S. Goundan, Isolation and characterization of chenopodin, the 11S seed storage protein of quinoa (*Chenopodium quinoa*), J. Agric. Food Chem. 41 (1993) 182–185, https://doi.org/10.1021/jf00026a006.
[16] AOAC, Cereal foods method 992.23, in: Patricia Cunnif (Ed.), Food Compos. Additives Nat. Contam. Off. Methods Anal. AOAC, 16th ed., AOAC, Maryland, 1996, p. 23.
[17] M.M. Bradford, A rapid and sensitive method for the quantitation of microgram quantities of protein utilizing the principle of protein-dye binding, Anal. Biochem. 72 (1976) 248–254, https://doi.org/10.1016/0003-2697(76)90527-3.
[18] U.K. Laemmli, Cleavage of structural proteins during the assembly of the head of bacteriophage T4, Nature 227 (1970) 680–685, https://doi.org/10.1038/227680a0.
[19] S.M. Kelly, T.J. Jess, N.C. Price, How to study proteins by circular dichroism, Biochim. Biophys. Acta – Proteins Proteomics 1751 (2005) 119–139, https://doi.org/10.1016/j.bbapap.2005.06.005.
[20] S.W. Provencher, J. Glöckner, Estimation of globular protein secondary structure from circular dichroism, Biochemistry 20 (1981) 33–37, https://doi.org/10.1021/bi00504a006.
[21] L. Whitmore, B.A. Wallace, Protein secondary structure analyses from circular dichroism spectroscopy: methods and reference databases, Biopolymers 89 (2008) 392–400, https://doi.org/10.1002/bip.20853.
[22] L. Whitmore, B.A. Wallace, DICHROWEB, an online server for protein secondary structure analyses from circular dichroism spectroscopic data, Nucl. Acids Res. 32 (2004) 668–673, https://doi.org/10.1093/nar/gkh371.
[23] A. Lobley, L. Whitmore, B.A. Wallace, DICHROWEB: an interactive website for the analysis of protein secondary structure from circular dichroism spectra, Bioinformatics 18 (2002) 211–212, https://doi.org/10.1093/bioinformatics/18.1.211.
[24] A. Kato, S. Nakai, Hydrophobicity determined by a fluorescence probe method and its correlation with surface properties of proteins, Biochim. Biophys. Acta – Protein Struct. 624 (1980) 13–20, https://doi.org/10.1016/0005-2795(80)90220-2.
[25] Y. Li, Z. Chen, H. Mo, Effects of pulsed electric fields on physicochemical properties of soybean protein isolates, LWT – Food Sci. Technol. 40 (2007) 1167–1175, https://doi.org/10.1016/j.lwt.2006.08.015.

[26] M. Cardamone, N.K. Puritt, Spectrofluorimetric assessment of the surface hydrophobicity of proteins, Boichem J. 282 (2000) 589–593.
[27] B.Y. Xiang, M.O. Ngadi, L.A. Ochoa-Martinez, M.V. Simpson, Pulsed electric field-induced structural modification of whey protein isolate, Food Bioprocess Technol. 4 (2011) 1341–1348, https://doi.org/10.1007/s11947-009-0266-z.
[28] S.A. Elsohaimy, T.M. Refaay, M.A.M. Zaytoun, Physicochemical and functional properties of quinoa protein isolate, Ann. Agric. Sci. 60 (2015) 297–305, https://doi.org/10.1016/j.aoas.2015.10.007.
[29] C.H. Tang, X.Y. Wang, X.Q. Yang, L. Li, Formation of soluble aggregates from insoluble commercial soy protein isolate by means of ultrasonic treatment and their gelling properties, J. Food Eng. 92 (2009) 432–437, https://doi.org/10.1016/j.jfoodeng.2008.12.017.
[30] M.E. Steffolani, P. Villacorta, E.R. Morales-Soriano, R. Repo-Carrasco, A.E. Leon, G.T. Perez, Physico-chemical, nutritional and functional characterization of protein isolated from different quinoa varieties (*Chenopodium quinoa* Willd), Igarss 2014 (54) (2014) 1–5, https://doi.org/10.1007/s13398-014-0173-7.2.
[31] F. Janssen, A. Pauly, I. Rombouts, K.J.A. Jansens, L.J. Deleu, J.A. Delcour, Proteins of amaranth (*Amaranthus spp.*), buckwheat (*Fagopyrum* spp.), and quinoa (Chenopodium spp.): a food science and technology perspective, Compr. Rev. Food Sci. Food Saf 16 (2017) 39–58, https://doi.org/10.1111/1541-4337.12240.
[32] Y.H. Chen, J.T. Yang, K.H. Chau, Determination of the helix and beta form of proteins in aqueous solution by circular dichroism, Biochemistry 13 (1974) 3350–3359, https://doi.org/10.1021/bi00713a027.
[33] O.E. Mäkinen, E. Zannini, P. Koehler, E.K. Arendt, Heat-denaturation and aggregation of quinoa (*Chenopodium quinoa*) globulins as affected by the pH value, Food Chem. 196 (2016) 17–24, https://doi.org/10.1016/j.foodchem.2015.08.069.
[34] M.F. Marcone, Y. Kakuda, R.Y. Yada, Salt soluble seed globulins of dicotyledonous and monocotyledonous plants II. Structural characterization, Food Chem. 63 (1998) 265–274, https://doi.org/10.1016/S0308-8146(97)00159-3.
[35] R. Navarro-Lisboa, C. Herrera, R.N. Zúñiga, J. Enrione, F. Guzmán, S. Matiacevich, C. Astudillo-Castro, Quinoa proteins (*Chenopodium quinoa* Willd.) fractionated by ultrafiltration using ceramic membranes: the role of pH on physicochemical and conformational properties, Food Bioprod. Process. 102 (2017) 20–30, https://doi.org/10.1016/j.fbp.2016.11.005.
[36] S.M. Choi, C.Y. Ma, Structural characterization of globulin from common buckwheat (*Fagopyrum esculentum* Moench) using circular dichroism and Raman spectroscopy, Food Chem. 102 (2007) 150–160, https://doi.org/10.1016/j.foodchem.2006.05.011.
[37] X. Chen, Y. Ru, F. Chen, X. Wang, X. Zhao, Q. Ao, FTIR spectroscopic characterization of soy proteins obtained through AOT reverse micelles, Food Hydrocolloids 31 (2013) 435–437, https://doi.org/10.1016/j.foodhyd.2012.11.017.
[38] Z. Wang, X.X. Sun, Z.X. Lian, X.X. Wang, J. Zhou, Z.S. Ma, The effects of ultrasonic/microwave assisted treatment on the properties of soy protein isolate/microcrystalline wheat-bran cellulose film, J. Food Eng. 114 (2013) 183–191, https://doi.org/10.1016/j.jfoodeng.2012.08.004.
[39] M. Carbonaro, P. Maselli, P. Dore, A. Nucara, Application of Fourier transform infrared spectroscopy to legume seed flour analysis, Food Chem. 108 (2008) 361–368, https://doi.org/10.1016/j.foodchem.2007.10.045.
[40] X.S. Qin, S.Z. Luo, J. Cai, X.Y. Zhong, S.T. Jiang, Y.Y. Zhao, Z. Zheng, Transglutaminase-induced gelation properties of soy protein isolate and wheat gluten mixtures with high intensity ultrasonic pretreatment, Ultrason. Sonochem. 31 (2016) 590–597, https://doi.org/10.1016/j.ultsonch.2016.02.010.
[41] C. Bruijnes, R. Bosman, P. Bareman, A. Besemer, Conformational analysis of starch derivatives by FTIR spectroscopy, Proc. SPIE 1145, 7th Intl Conf on Fourier Transform Spectroscopy 1145, 1989, pp. 342–344, , https://doi.org/10.1117/12.969491.
[42] V. Nowak, J. Du, U.R. Charrondière, Assessment of the nutritional composition of quinoa (*Chenopodium quinoa* Willd.), Food Chem. 193 (2016) 47–54, https://doi.org/10.1016/j.foodchem.2015.02.111.
[43] J. Ruales, B.M. Nair, Quinoa (*Chenopodium quinoa*, Willd) seeds, Plant Foods Hum. Nutr. 45 (1994) 223–246, https://doi.org/10.1007/BF01094092.
[44] S. Bou, S. Bel, A. Magnin, F. Pignon, M. Impéror-clerc, Ultrasonic assisted production of starch nanoparticles: structural characterization and mechanism of disintegration, Ultrason. Sonochem. 41 (2017) 327–336, https://doi.org/10.1016/j.ultsonch.2017.09.033.
[45] I. Majid, G.A. Nayik, V. Nanda, Ultrasonication and food technology: a review, Cogent Food Agric. 20 (2015) 1–11, https://doi.org/10.1080/23311932.2015.1071022.
[46] K.K. Turoverov, I.M. Kuznetsova, Intrinsic fluorescence of actin, J. Fluoresc. 13 (2003) 41–57, https://doi.org/10.1023/A:1022366816812.
[47] C.-H. Tang, X.-Q. Yang, Z. Chen, H. Wu, Z. Peng, Physicochemical and structural characteristics of sodium caseinate biopolymers induce by microbial transglutaminase, J. Food Biochem. 29 (2005) 402–421, https://doi.org/10.1111/j.1745-4514.2005.00038.x.
[48] E. Burstein, N. Vedenkina, M. Ivkova, Tryptophan residues in protein molecules, Photochem. Photobiol. 18 (1973) 263–279, https://doi.org/10.1111/j.1751-1097.1973.tb06422.x.
[49] J.T. Vivian, P.R. Callis, Mechanisms of tryptophan fluorescence shifts in proteins, Biophys. J. 80 (2001) 2093–2109, https://doi.org/10.1016/S0006-3495(01)76183-8.
[50] S.S. Komath, M.J. Swamy, Fluorescence quenching, time-resolved fluorescence and chemical modification studies on the tryptophan residues of snake gourd (*Trichosanthes anguina*) seed lectin, J. Photochem. Photobiol. B: Biol. 50 (1999) 108–118, https://doi.org/10.1016/S1011-1344(99)00079-2.
[51] A.R. Jambrak, V. Lelas, T.J. Mason, G. Krešić, M. Badanjak, Physical properties of ultrasound treated soy proteins, J. Food Eng. 93 (2009) 386–393, https://doi.org/10.1016/j.jfoodeng.2009.02.001.
[52] B. Karki, B.P. Lamsal, D. Grewell, A.L. Pometto, J. Van Leeuwen, S.K. Khanal, S. Jung, Functional properties of soy protein isolates produced from ultrasonicated defatted soy flakes, JAOCS J. Am. Oil Chem. Soc. 86 (2009) 1021–1028, https://doi.org/10.1007/s11746-009-1433-0.
[53] C.P. O'Donnell, B.K. Tiwari, P. Bourke, P.J. Cullen, Effect of ultrasonic processing on food enzymes of industrial importance, Trends Food Sci. Technol. 21 (2010) 358–367, https://doi.org/10.1016/j.tifs.2010.04.007.
[54] L. Zhang, L.J. Wang, W. Jiang, J.Y. Qian, Effect of pulsed electric field on functional and structural properties of canola protein by pretreating seeds to elevate oil yield, LWT – Food Sci. Technol. 84 (2017) 73–81, https://doi.org/10.1016/j.lwt.2017.05.048.
[55] L. Stryer, The interaction of a naphthalene dye with apomyoglobin and apohemoglobin: a fluorescent probe of non-polar binding sites, J. Mol. Biol. 13 (1965) 482–495, https://doi.org/10.1016/S0022-2836(65)80111-5.
[56] B. Zhang, D. Yuan, X. He, X. Yang, Z. Gao, J. Wang, Physiochemical and conformational properties of soluble aggregates from soy protein isolates mediated by hydrothermal cooking: a comparative study with moisture heat treatment, J. Food Technol. 1 (2016) 1–9, https://doi.org/10.18689/mjft.2016-101.
[57] A. Hawe, M. Sutter, W. Jiskoot, Extrinsic fluorescent dyes as tools for protein characterization, Pharm. Res. 25 (2008) 1487–1499, https://doi.org/10.1007/s11095-007-9516-9.
[58] H. Mach, D.B. Volkin, C.J. Burke, C.R. Middaugh, Ultraviolet absorption spectroscopy, Methods Mol. Biol. 40 (1995) 91–114, https://doi.org/10.1385/0-89603-301-5:91.
[59] F. Schmid, Biological macromolecules: spectrophotometry concentrations, Encycl. Life Sci. (2001) 1–4.
[60] C. Valenzuela, L. Abugoch, C. Tapia, A. Gamboa, Effect of alkaline extraction on the structure of the protein of quinoa (*Chenopodium quinoa* Willd.) and its influence on film formation, Int. J. Food Sci. Technol. 48 (2013) 843–849, https://doi.org/10.1111/ijfs.12035.
[61] G.A. Ruiz, M. Opazo-Navarrete, M. Meurs, M. Minor, G. Sala, M. van Boekel, M. Stieger, A.E.M. Janssen, Denaturation and in vitro gastric digestion of heat-treated quinoa protein isolates obtained at various extraction pH, Food Biophys. 11 (2016) 184–197, https://doi.org/10.1007/s11483-016-9429-4.
[62] L. Abugoch, E. Castro, C. Tapia, M.C. Añón, P. Gajardo, A. Villarroel, Stability of quinoa flour proteins (*Chenopodium quinoa* Willd.) during storage, Int. J. Food Sci. Technol. 44 (2009), https://doi.org/10.1111/j.1365-2621.2009.02023.x.
[63] C. Valenzuela, L. Abugoch, C. Tapia, A. Gamboa, Effect of alkaline extraction on the structure of the protein of quinoa (*Chenopodium quinoa* Willd.) and its influence on film formation, Int. J. Food Sci. Technol. 48 (2013), https://doi.org/10.1111/ijfs.12035.
[64] M.R.B. Balzotti, J.N. Thornton, P.J. Maughan, D.A. Mcclellan, M.R. Stevens, E.N. Jellen, D.J. Fairbanks, C.E. Coleman, Expression and evolutionary relationships of the chenopodium quinoa 11S seed storage protein gene, Int. J. Plan Sci. 169 (2008) 281–291, https://doi.org/10.1086/523874.
[65] M.A. Malik, H.K. Sharma, C.S. Saini, High intensity ultrasound treatment of protein isolate extracted from dephenolized sun flower meal: Effect on physicochemical and functional properties, Ultrason. Sonochem. 39 (2017) 511–519, https://doi.org/10.1016/j.ultsonch.2017.05.026.
[66] B. Karki, Use of high-power ultrasound during soy protein production and study of its effect on functional properties of soy protein isolate (Graduate Theses and Dissertations), 1055, 2009. http://lib.dr.iastate.edu/etd/11055.
[67] J.M. Hughes, P.M. Budd, A. Grieve, P. Dutta, K. Tiede, J. Lewis, Highly Monodisperse, Lanthanide-containing Polystyrene Nanoparticles as Potential Standard Reference Materials for Environmental "Nano" Fate Analysis, 42061, 2015, https://doi.org/10.1002/app.42061.
[68] R.N. Garcia, R.V. Arocena, A.C. Laurena, E.M. Tecson-Mendoza, 11S and 7S globulins of coconut (*Cocos nucifera* L.): purification and characterization, J. Agric. Food Chem. 53 (2005) 1734–1739, https://doi.org/10.1021/jf0402173.
[69] L. Jiang, J. Wang, Y. Li, Z. Wang, J. Liang, R. Wang, Y. Chen, W. Ma, B. Qi, M. Zhang, Effects of ultrasound on the structure and physical properties of black bean protein isolates, Food Res. Int. 62 (2014) 595–601, https://doi.org/10.1016/j.foodres.2014.04.022.